
A GENERAL FRAMEWORK FOR MULTI-STEP AHEAD ADAPTIVE CONFORMAL HETEROSCEDASTIC TIME SERIES FORECASTING *

Martim Sousa

IEETA/DETI, University of Aveiro
martimsousa@ua.pt

Ana Maria Tomé

IEETA/DETI, University of Aveiro
ana@ua.pt

José Moreira

IEETA/DETI, University of Aveiro
jose.moreira@ua.pt

ABSTRACT

The exponential growth of machine learning (ML) has prompted a great deal of interest in quantifying the uncertainty of each prediction for a user-defined level of confidence. Reliable uncertainty quantification is crucial and is a step towards increased trust in AI results. It becomes especially important in high-stakes decision-making, where the true output must be within the confidence set with high probability. Conformal prediction (CP) is a distribution-free uncertainty quantification framework that works for any black-box model and yields prediction intervals (PIs) that are valid under the mild assumption of exchangeability. CP-type methods are gaining popularity due to being easy to implement and computationally cheap; however, the exchangeability assumption immediately excludes time series forecasting. Although recent papers tackle covariate shift, this is not enough for the general time series forecasting problem of producing H-step ahead valid PIs. To attain such a goal, we propose a new method called AEnbMIMOCQR (Adaptive ensemble batch multi-input multi-output conformalized quantile regression), which produces asymptotic valid PIs and is appropriate for heteroscedastic time series. We compare the proposed method against state-of-the-art competitive methods in the NN5 forecasting competition dataset. All the code and data to reproduce the experiments are made available.

Keywords Conformal prediction · Conformalized quantile regression · Conformal time series forecasting · Covariate shift · Multi-step ahead forecasting

1 Introduction

In a time series forecasting problem, given the past observations $[x_{n-d+1}, \dots, x_n]$ the goal is to predict the next observations $[x_{n+1}, x_{n+2}, \dots, x_{n+H}]$, where H is the number of steps to predict, also known as the horizon; and d is the number of lags. Unfortunately, when it comes to practical deployments, the forecasts $[\hat{x}_{n+1}, \hat{x}_{n+2}, \dots, \hat{x}_{n+H}]$ have an unknown associated uncertainty given by

$$\epsilon_{n+h} = x_{n+h} - \hat{x}_{n+h}, \quad \forall h \in \{1, 2, \dots, H\}. \quad (1)$$

**Remark:* This is a preprint whose final form is not yet published.

Therefore, throughout this article, we focus on building PIs around each forecast that faithfully assesses the said uncertainty of the ML model for a user-defined level of confidence. Table (1) contains the notation used throughout this article.

Notation	Meaning
α	Miscoverage rate α
$\hat{C}_{1-\alpha}(\mathbf{x}_n)$	$1 - \alpha$ PI on input x_n
$\hat{C}_{1-\alpha}^{(t)}(\mathbf{x}_n)$	$1 - \alpha$ PI on input x_n and timestep t
$x_{1:d}$	Compact version of (x_1, \dots, x_d)
x	a scalar
\mathbf{x}	a vector
X	a matrix or a probability distribution (easily distinguished)
\mathbf{X}	a tensor

Table 1: Notation used throughout this article.

Inductive conformal prediction (ICP) is a distribution-free uncertainty quantification technique that aims to give *valid* PIs in the sense of Theorem (1.1) [1, 2, 3, 4]. Unlike full conformal prediction [1], ICP, also known as *split conformal prediction*, uses a calibration set \mathcal{D}_{cal} to compute $\{(s_i)\}_{i=1}^{n_{cal}}$ *non-conformity scores*. Usually, in the interest of space, ICP is preferred over full conformal prediction. The aforementioned scores are calculated using a *non-conformity score function* $s(\mathbf{x}, y)$, which works as a heuristic notion of uncertainty, where larger scores encode worse agreement between the input \mathbf{x} and true output y . Thereafter, we compute $\hat{q} = \text{Quantile}(\{(s_i)\}_{i=1}^{n_{cal}}; 1 - \alpha)$ and rely on this information to get PIs on new data, here exemplified by \mathcal{D}_{val} . Even though ICP works for any *non-conformity score function* s , as stated in Theorem (1.1), the choice of this function has a direct impact on the PIs width. From a practical point of view, we want *valid* PIs with the shortest possible width to be informative in common decision-making tasks. Ideally, we also seek conditional coverage given by Eq.(4). Obviously, conditional coverage implies marginal coverage, while the reciprocal is not true. Conditional coverage is proved impossible with ICP; however, we can heuristically approximate it. Note that conditional coverage is an important property as we want PIs to adapt to heteroscedasticity.

Definition 1 (Exchangeability). *A sequence of random variables $Z_1, Z_2, \dots, Z_n \in \mathcal{Z}$ are exchangeable if and only if for any permutation $\pi : \{1, 2, \dots, n\} \rightarrow \{1, 2, \dots, n\}$ and every measurable set $E \subseteq \mathcal{Z}^n$, we have*

$$\mathbb{P}\{(Z_1, Z_2, \dots, Z_n) \in E\} = \mathbb{P}\{(Z_{\pi(1)}, Z_{\pi(2)}, \dots, Z_{\pi(n)}) \in E\} \quad (2)$$

Theorem 1.1 (Marginal coverage guarantee). *Suppose that $\mathcal{D} = \{(\mathbf{x}_i, y_i)\}_{i=1}^N$ are exchangeable samples, if we construct $\hat{C}_{1-\alpha}(\mathbf{x}_{val})$ using ICP, the following inequality holds for any non-conformity score function s and any $\alpha \in (0, 1)$*

$$\mathbb{P}(y_{val} \in \hat{C}_{1-\alpha}(\mathbf{x}_{val})) \geq 1 - \alpha. \quad (3)$$

Proof. See [1]. □

Definition 2 (Conditional coverage). *An ICP procedure guarantees conditional coverage if*

$$\mathbb{P}(y_{val} \in \hat{C}_{1-\alpha}(\mathbf{x}_{val}) | X = \mathbf{x}_{val}) \geq 1 - \alpha. \quad (4)$$

Recalling our time series forecasting problem, we easily verify that ICP methods cannot be applied directly to time series because the exchangeability assumption does not hold. Distribution changes over time. Therefore, we rather focus on an online conformal setting as in [5, 6, 7] that achieves *asymptotic validity*.

Definition 3 (Asymptotic valid PIs). *Let $\hat{C}_{1-\alpha}^{(t)}(x_{n+h})$ be the PI for x_{n+h} with $1 - \alpha$ confidence at timestep t . These PIs are said asymptotic valid if*

$$\lim_{T \rightarrow \infty} \frac{1}{T} \sum_{t=1}^T \mathbb{1}\{x_{n+h} \in \hat{C}_{1-\alpha}^{(t)}(x_{n+h})\} = 1 - \alpha, \quad \forall h \in \{1, 2, \dots, H\}, \quad (5)$$

where $\hat{C}_{1-\alpha}^{(t)}(x_{n+h}) = [\hat{x}_{n+h}^L, \hat{x}_{n+h}^U]$, with \hat{x}_{n+h}^L being a lower bound for x_{n+h} and \hat{x}_{n+h}^U an upper bound; $\mathbb{1}$ denotes the indicator function.

Article outline

The article outline is as follows. Section 2 reviews two forecasting strategies that we will utilize, one for single-output models; and another for multi-output ones. Section 3 provides an overview of related work which inspired the proposed method. Section 4 introduces our approach called AEnbMIMOCQR. Section 5 compares the effectiveness of our method against state-of-the-art online conformal frameworks in the NN5 forecasting competition dataset. Finally, Section 6 draws main conclusions.

2 Forecasting strategies

Whenever dealing with an H -step ahead forecasting problem, we must decide which forecasting strategy to use. Although this is a vast active research topic that goes beyond the scope of this article, we will introduce two well-known methods for this purpose: the recursive strategy; and the multi-input multi-output (MIMO) to forecast each observation of the desired horizon [8, 9].

2.1 Recursive strategy

Let $\hat{f} : \mathbb{R}^d \rightarrow \mathbb{R}$ denote a ML model that predicts the next observation based on d lags. In the recursive strategy, each forecast of the horizon H is computed through the following equations

$$\hat{x}_{n+h} = \begin{cases} \hat{f}(x_{n-d+1}, \dots, x_n), & \text{for } h = 1, \\ \hat{f}(x_{n-d+h}, \dots, x_n, \hat{x}_{n+1}, \dots, \hat{x}_{n+h-1}), & \text{for } h \in \{2, \dots, d\}, \\ \hat{f}(\hat{x}_{n+h-d}, \dots, \hat{x}_{n+h-1}), & \text{for } h \in \{d+1, \dots, H\}. \end{cases}$$

The major shortcoming of this approach is that we trained the ML model \hat{f} on d actual lag values, yet in the forecasting process, we include previous forecasts as inputs, hence accumulating errors as h increases. Note that for $h > d$ the input only contains forecasts.

2.2 MIMO

In the MIMO strategy, we train a ML model $\hat{F} : \mathbb{R}^d \rightarrow \mathbb{R}^H$ that directly learns how to forecast each observation of the horizon. Therefore, this strategy has no accumulation of errors as we forecast each observation of the horizon in one step as

$$\hat{F}(x_{n-d+1}, \dots, x_n) = [\hat{x}_{n+1}, \dots, \hat{x}_{n+H}]. \quad (6)$$

However, the underlying structure is more complex and thus harder to learn in comparison to the recursive strategy. Furthermore, few models besides neural networks can cope with multi-output regression tasks. Most of the ML models are optimized for a single target.

3 Related work

In this section, we do a brief recap on competitive methods for probabilistic forecasting that inspired our method and address their drawbacks.

3.1 Probabilistic forecasting with ARIMA

ARIMA(d, d^*, q) models are still among the most robust and best performing methods for time series forecasting [10]. PIs can be obtained from ARIMA(d, d^*, q) models as

$$\hat{C}_{1-\alpha}(x_{n+h}) = [\hat{x}_{n+h} - c_{1-\alpha}\hat{\sigma}_h, \hat{x}_{n+h} + c_{1-\alpha}\hat{\sigma}_h], \quad \forall h \in \{1, 2, \dots, H\}, \quad (7)$$

where \hat{x}_{n+h} is the h -step ahead *point prediction*; $c_{1-\alpha}$ is a constant whose value is the inverse cumulative distribution of the standard normal distribution calculated on $1 - \alpha$; and $\hat{\sigma}_h$ is the h -step ahead estimation of the standard deviation.

Nevertheless, the standard deviation estimation is obtained from the model residuals, which are assumed to be serially uncorrelated and normally distributed. If both assumptions are not met, these PIs become unreliable. Moreover, $\hat{\sigma}_h$ is optimized for marginal coverage, hence it does not change from the joint input (lags).

Furthermore, (Hyndman & Athanasopoulos, 2018) [11] leave an interesting remark. If $d^* = 0$, then the time series is deemed stationary, and thus $\hat{\sigma}_h$ does not change for every $h \in \{1, \dots, H\}$, while if $d^* \geq 1$, it has tendency and therefore PIs width increase over time.

3.2 EnbPI algorithm

The EnbPI algorithm, summarized in Algorithm (1), is a framework gaining popularity that achieves *asymptotic validity* and does not require data splitting. It assumes that the samples $(x_{(n_t-d+1):n_t}, x_{n_t+1})$ come from the following process

$$x_{n_t+1} = f(x_{(n_t-d+1):n_t}) + \epsilon_t, \quad t = 1, 2, \dots \quad (8)$$

where $n_t = d + t - 1$.

The goal is to approximate the real unknown function $f : \mathbb{R}^d \rightarrow \mathbb{R}$ with a regression model $\hat{f} : \mathbb{R}^d \rightarrow \mathbb{R}$. For this purpose, we compute a *leave-one-out* homogeneous ensemble estimator \hat{f}_t that excludes the t -th training sample. Each in-sample residual $\epsilon_t^\phi = |x_{n_t+1} - \hat{f}_t^\phi(x_{(n_t-d+1):n_t})|$ is added to a *non-conformity set* ϵ and therefore PIs come in the following form

$$\hat{C}_{1-\alpha}^{(t)}(x_{n_t+1}) = [\hat{f}_t^\phi(x_{(n_t-d+1):n_t}) - \omega_t^\phi, \hat{f}_t^\phi(x_{(n_t-d+1):n_t}) + \omega_t^\phi], \quad (9)$$

where ω_t^ϕ is the $(1 - \alpha)$ quantile of ϵ up to t ; and the function ϕ is an aggregation function such as the mean, median, trimmed mean, etc.

Up to this point, this method seems not to differ much from ICP regression methods. The cleverness of this algorithm lies within the batch size H that makes this method dynamic and *asymptotic valid*. The *non-conformity set* ϵ works as a sliding window, after H -step ahead forecasts, the first H *non-conformity scores* are discarded, and the most recent H are added, thus making it dynamic. The batch size H controls how fast the algorithm adapts. If $H = 1$, the *non-conformity set* is renewed after each forecast, whereas if $H = \infty$, it never updates.

Algorithm 1 EnbPI algorithm adapted to recursive H -step ahead forecasting. [12]

Input: Training data $\{(x_{(n_i-d+1):n_i}, x_{n_i+1})\}_{i=1}^T$, regression model $\hat{f} : \mathbb{R}^d \rightarrow \mathbb{R}$, miscoverage rate α , aggregation function ϕ , number of bootstrap models B , the batch size H , and test data $\{(x_{(n_t-d+1):n_t}, x_{n_t+1})\}_{t=T+1}^{T+T_1}$, with x_{n_t+1} revealed only after the batch of s prediction intervals with t in the batch are constructed.

Output: Ensemble prediction intervals $\{\hat{C}_{1-\alpha}^{(t)}(x_{n_t+1})\}_{t=T+1}^{T+T_1}$

```

1: for  $b=1, \dots, B$  do
2:   Sample an index set  $S_b = (i_1, \dots, i_T)$  from indices  $(1, \dots, T)$ 
3:   Compute  $\hat{f}^b \leftarrow \hat{f}(\{(x_{(n_i-d+1):n_i}, x_{n_i+1}) \mid i \in S_b\})$ 
4: end for
5: Initialize  $\epsilon \leftarrow \{\}$ 
6: for  $i \leftarrow 1, \dots, T$  do
7:    $\hat{f}_{-i}^\phi(x_{(n_i-d+1):n_i}) \leftarrow \phi(\{\hat{f}^b(x_{(n_i-d+1):n_i}) \mid i \notin S_b\})$ 
8:   Compute  $\epsilon_i^\phi \leftarrow |x_{n_i+1} - \hat{f}_{-i}^\phi(x_{(n_i-d+1):n_i})|$ 
9:    $\epsilon \leftarrow \epsilon \cup \{\epsilon_i^\phi\}$ 
10: end for
11: for  $t \leftarrow T+1, \dots, T+T_1$  do
12:   Compute  $(\hat{x}_{(n_t-d+1):n_t})$  with the recursive strategy formula (see (2.1)) for  $h = t - T \bmod H$ 
13:   Let  $\hat{f}_{-t}^\phi(\hat{x}_{(n_t-d+1):n_t}) \leftarrow \phi(\{\hat{f}^b(\hat{x}_{(n_t-d+1):n_t})\}_{b=1}^B)$ 
14:   Let  $\omega_t^\phi \leftarrow (1 - \alpha)$  quantile of  $\epsilon$ 
15:   Return  $\hat{C}_{1-\alpha}^{(t)} \leftarrow [\hat{f}_{-t}^\phi(\hat{x}_{(n_t-d+1):n_t}) - \omega_t^\phi, \hat{f}_{-t}^\phi(\hat{x}_{(n_t-d+1):n_t}) + \omega_t^\phi]$ 
16:   if  $t - T \equiv 0 \bmod H$  then
17:     for  $j \leftarrow t - H, \dots, t - 1$  do
18:       Compute  $\epsilon_j^\phi \leftarrow |x_{n_j+1} - \hat{f}_{-j}^\phi(\hat{x}_{(n_j-d+1):n_j})|$ 
19:        $\epsilon \leftarrow (\epsilon - \{\epsilon_1^\phi\}) \cup \{\epsilon_j^\phi\}$  and reset index of  $\epsilon$ 
20:     end for
21:   end if
22: end for

```

We further explore the theoretical analysis of EnbPI to explain why despite being *asymptotic valid*, as shown in [12], it may take a long time before EnbPI starts producing valid PIs for time series forecasting.

Lemma 3.1. *Let B be the number of bootstrap models of EnbPI with T training samples, then the length of the non-conformity set ϵ is equal to $T \left(1 - \left(1 - \left(1 - \frac{1}{T}\right)^T\right)^B\right) \approx T \left(1 - \left(1 - e^{-1}\right)^B\right)$ on average.*

Proof. We know that the probability of an index not belonging to a bootstrap index set is equal to

$$\mathbb{P}(i \notin S_b) = \left(1 - \frac{1}{T}\right)^T. \quad (10)$$

Since

$$\lim_{T \rightarrow \infty} \left(1 - \frac{1}{T}\right)^T = e^{-1}, \quad (11)$$

then for a large enough T , $\left(1 - \frac{1}{T}\right)^T \approx e^{-1}$. Let X_i be the distribution that represents the number of *leave-one-out* bootstrap models used to compute \hat{f}_i^ϕ . We know that $X_i \sim \text{Bin}(B, \left(1 - \frac{1}{T}\right)^T)$ and so

$$\mathbb{P}(X_i \geq 1) = 1 - \mathbb{P}(X_i = 0) = 1 - \left(1 - \left(1 - \frac{1}{T}\right)^T\right)^B \quad (12)$$

From here, follows that the length distribution of ϵ denoted by $L \sim \text{Bin}(T, 1 - \left(1 - \left(1 - \frac{1}{T}\right)^T\right)^B)$ and therefore

$$\mathbb{E}(L) = T \left(1 - \left(1 - \left(1 - \frac{1}{T}\right)^T\right)^B\right) \approx T \left(1 - \left(1 - e^{-1}\right)^B\right). \quad (13)$$

□

An immediate consequence of Lemma (3.1) is that

$$\lim_{B \rightarrow \infty} T \left(1 - \left(1 - e^{-1}\right)^B\right) = T(1 - 0) = T \quad (14)$$

Consequently, the length of the *non-conformity set* ϵ may be roughly approximated by T for large enough T and B .

Lemma 3.2. *Let $N = |\epsilon|$, i.e., the non-conformity set length. If we use the recursive strategy with a regression model $\hat{f} : \mathbb{R}^d \rightarrow \mathbb{R}$, then only after $\max\{N, d\} + k$ forecasting steps the non-conformity set ϵ does not contain any in-sample *leave-one-out* ensemble non-conformity score and contains at least a cycle of accumulation of errors associated with the recursive strategy, where $k = \max\{N, d\} \bmod H$.*

Proof. Follows immediately from the recursive strategy definition (see (2.1)) and Algorithm (1). □

Lemmas (3.1) and (3.2) bring important results to explain why the EnbPI algorithm has some pitfalls for time series forecasting PIs, despite being *asymptotic valid*. Given the rough approximation of the *non-conformity set* ϵ length T , by applying Lemma (3.2), then only after $\max\{T, d\} + k$ forecasting steps the *non-conformity set* is adapted to the accumulation of errors associated with the recursive strategy and none in-sample *leave-one-out* ensemble *non-conformity score* is in the *non-conformity set* ϵ , where $k = \max\{N, d\} \bmod H$. In other words, EnbPI computes in-sample *leave-one-out* ensemble *non-conformity scores* as (line 8 of Algorithm (1))

$$\epsilon_i^\phi = |x_{n_i+1} - \hat{f}_{-i}^\phi(x_{(n_i-d+1):n_i})| \quad (15)$$

However, these in-sample *leave-one-out* ensemble *non-conformity scores* are computed using d actual lags as joint input and thus it does not faithfully reflect the true forecast uncertainty since in the out-of-sample phase the joint input incorporates lags that are previous forecasts and therefore uncertain. To conclude, Lemma (3.2) gives what can be considered a warm-up period before EnbPI produces reliable PIs for time series forecasting.

Remarks

- If the in-sample *leave-one-out* ensemble *non-conformity score* (ϵ) length is too high we can speed up convergence by sampling without replacement a fraction of observations from ϵ .
- This method is not adaptive to heteroscedasticity, i.e., PIs width is always equal to $2\omega_t^\phi$ within the same batch.

3.3 Conformalized quantile regression

Conformalized quantile regression (CQR) is a procedure that inherits the advantages of quantile regression (QR) and CP [13, 14, 15, 16]. The idea is to use QR to get an estimation of the true unknown conditional quantiles from the data and then apply CP to ensure marginal coverage in finite samples. Consequently, we get PIs that are adaptive to heteroscedasticity due to QR, i.e., PIs vary accordingly to the input \mathbf{x} and also marginal coverage because of CP.

Recall that the τ -quantile of a conditional distribution $Y|X$ calculated on $X = \mathbf{x}$ is given by

$$Q_\tau(\mathbf{x}) = \inf \{y \in \mathbb{R} : F(y|X = \mathbf{x}) \geq \tau\}. \quad (16)$$

Likewise, if $F(y|X = \mathbf{x})$ has an inverse since it is an increasing function, we also get

$$Q_\tau(\mathbf{x}) = F^{-1}(\tau|X = \mathbf{x}) \quad (17)$$

QR aims to approximate $Q_{\alpha/2}(\mathbf{x})$ and $Q_{1-\alpha/2}(\mathbf{x})$ to get a lower and upper bound, respectively, that approximate conditional coverage. This is achieved by simply replacing the common squared error loss with a quantile loss, also known as *pinball loss* formulated as

$$\rho_\tau(y, \mathbf{x}, \hat{f}) = \max \left(\tau(y - \hat{f}(\mathbf{x})), ((\tau - 1)(y - \hat{f}(\mathbf{x}))) \right), \quad (18)$$

Hence, we attempt to minimize the following objective

$$\min \sum_{i=1}^{n_{train}} \rho_\tau(\hat{f}(\mathbf{x}_i), y_i) + \Omega(\boldsymbol{\theta}), \quad (19)$$

where $\Omega(\boldsymbol{\theta})$ is a potential regularizer; and $\hat{f} : \mathbb{R}^d \rightarrow \mathbb{R}$ any black-box regression model.

However, in finite samples, we only get estimates $\hat{Q}_{\alpha/2}(\mathbf{x})$ and $\hat{Q}_{1-\alpha/2}(\mathbf{x})$ after minimizing Eq.(19) that frequently do not attain marginal coverage. Therefore, (Romano et al., 2019) [14] had the brilliant idea of applying CP on top of QR via the following *non-conformity score function*

$$s(\mathbf{x}, y) = \max \{ \hat{Q}_{\alpha/2}(\mathbf{x}) - y, y - \hat{Q}_{1-\alpha/2}(\mathbf{x}) \}. \quad (20)$$

We use the aforementioned *non-conformity score function* on a calibration set and then compute

$$\hat{q} = \text{Quantile}(\{(s_i)\}_{i=1}^{n_{cal}}; 1 - \alpha), \quad (21)$$

to get PIs as

$$[\hat{Q}_{\alpha/2}(\mathbf{x}) - \hat{q}, \hat{Q}_{1-\alpha/2}(\mathbf{x}) + \hat{q}], \quad (22)$$

which attain marginal coverage and approximately conditional coverage.

3.4 EnbCQR algorithm

EnbCQR [17] follows the EnbPI algorithm structure (see Algorithm (1)), yet it uses CQR instead of using the absolute errors as the *non-conformity score function* ($\epsilon_i^\phi = |x_{n_i+1} - \hat{f}_{-i}^\phi(x_{(n_i-d+1):n_i})|$) to adapt to heteroscedastic time series.

3.5 MIMOCQR algorithm

In a slightly different direction, several papers group observations in a MIMO block structure which preserves dependence as $B_t = (x_{(n_t-d+1):n_t}, x_{(n_t+1):(n_t+H)})$ [18, 19]. Therefore, under the exchangeability assumption of those blocks (see Definition (1)) it is possible to apply conformal inference. Algorithm (2) encompasses every step to do so.

Suppose that $\hat{F}_{\alpha/2} : \mathbb{R}^d \rightarrow \mathbb{R}^H$ and $\hat{F}_{1-\alpha/2} : \mathbb{R}^d \rightarrow \mathbb{R}^H$ are two multi-output QR models that yield a multi-output lower bound and upper bound, respectively. Consequently, to achieve marginal coverage in finite samples, the following vector *non-conformity score function* version of Eq.(20) must be utilized

$$\mathbf{s}(x_{(n_t-d+1):n_t}, x_{(n_t+1):(n_t+H)}) = \max \{ \hat{F}_{\alpha/2}(x_{(n_t-d+1):n_t}) - x_{(n_t+1):(n_t+H)}, x_{(n_t+1):(n_t+H)} - \hat{F}_{1-\alpha/2}(x_{(n_t-d+1):n_t}) \}. \quad (23)$$

Thereby, let ϵ_h denote the resulting *non-conformity scores* after applying Eq.(23) on a holdout set for the h -step ahead forecast, then

$$\hat{q}^{(h)} = \text{Quantile}(\epsilon_h; 1 - \alpha), \quad \forall h \in \{1, \dots, H\}, \quad (24)$$

and therefore PIs come as

$$[\hat{F}_{\alpha/2}(x_{(n_t-d+1):n_t}) - \hat{q}, \hat{F}_{1-\alpha/2}(x_{(n_t-d+1):n_t}) + \hat{q}], \quad (25)$$

where $\hat{q} = \bigcup_{h=1}^H \{\hat{q}^{(h)}\}$.

This method circumvents the accumulation of errors associated with recursive EnbPI and EnbCQR by employing the MIMO strategy; however, as we will later discuss, the distribution of blocks usually shifts over time, culminating in decreasing coverage. Therefore, we must draw some ideas from dynamic methods as EnbPI and EnbCQR and adaptive conformal inference, introduced in the upcoming subsection.

Algorithm 2 Multi-input multi-output conformalized quantile regression (MIMOCQR)

Input: A training set $\{(B_i := x_{(n_i-d+1):n_i}, x_{(n_i+1):(n_i+H)})\}_{i=1}^T$, miscoverage rate α , a multi-output QR model $\hat{F}_T : \mathbb{R}^d \rightarrow \mathbb{R}^H$, a test set $\{(x_{(n_t-d+1):n_t}, x_{(n_t+1):(n_t+H)})\}_{t=T+1}^{T+T_1}$

Output: PIs $\{\hat{C}_{1-\alpha}^{(t)}(x_{(n_t+1):(n_t+H)})\}_{t=T+1}^{T+T_1}$

```

1: Sample an index set  $S_b = (i_1, \dots, i_T)$  from indices  $(1, \dots, T)$ 
2: Compute  $[\hat{F}_{\alpha/2}, \hat{F}_{1-\alpha/2}] \leftarrow (\hat{F}_{\alpha/2}(\{(B_i) \mid i \in S_b\}), \hat{F}_{1-\alpha/2}(\{(B_i) \mid i \in S_b\}))$ 
3:  $\epsilon_h \leftarrow \{\}$ ,  $\forall h \in \{1, \dots, H\}$ 
4: for  $i \leftarrow 1, \dots, T$  do
5:   if  $i \notin S_b$  then
6:      $[\hat{x}_{n_i+1}^L, \dots, \hat{x}_{n_i+H}^L] \leftarrow \hat{F}_{\alpha/2}(x_{n_i-d+1}, \dots, x_{n_i})$ 
7:      $[\hat{x}_{n_i+1}^U, \dots, \hat{x}_{n_i+H}^U] \leftarrow \hat{F}_{1-\alpha/2}(x_{n_i-d+1}, \dots, x_{n_i})$ 
8:     Compute  $\epsilon_h \leftarrow \epsilon_h \cup \{\max\{\hat{x}_{n_i+h}^L - x_{n_i+h}, x_{n_i+h} - \hat{x}_{n_i+h}^U\}\}, \quad \forall h \in \{1, \dots, H\}$ 
9:   end if
10: end for
11: Compute  $\hat{q}^{(h)} \leftarrow \text{Quantile}(\epsilon_h; 1 - \alpha), \forall h \in \{1, \dots, H\}$ 
12: for  $t \leftarrow T + 1, \dots, T + T_1$  do
13:    $[\hat{x}_{n_t+1}^L, \dots, \hat{x}_{n_t+H}^L] \leftarrow \hat{F}_{\alpha/2}(x_{n_t-d+1}, \dots, x_{n_t})$ 
14:    $[\hat{x}_{n_t+1}^U, \dots, \hat{x}_{n_t+H}^U] \leftarrow \hat{F}_{1-\alpha/2}(x_{n_t-d+1}, \dots, x_{n_t})$ 
15:   Return  $\hat{C}_{1-\alpha}^{(t)}(x_{(n_t+1):(n_t+H)}) \leftarrow [\hat{x}_{n_t+h}^L - \hat{q}^{(h)}, \hat{x}_{n_t+h}^U + \hat{q}^{(h)}], \quad \forall h \in \{1, \dots, H\}$ 
16: end for
```

3.6 Adaptive conformal inference

Adaptive conformal inference (ACI) [6] is another method whose goal is to cope with distribution shift problems. However, it relies on a different philosophy compared to the former methods. Instead of having a fixed α , we use a time-varying $(\alpha_t)_{t \in \mathbb{N}}$ updated via the following equation

$$\alpha_{t+1} = \alpha_t + \gamma(\alpha_t - \mathbb{1}\{y_t \in \hat{C}_{1-\alpha}^{(t)}(x_t)\}). \quad (26)$$

The method starts with $\alpha_1 = \alpha$, and γ works as a learning rate that controls how fast we desire the conformal method to adapt. Although the choice of γ has been improved in [7], the minor problem of this method is that $\forall t \in \mathbb{N}$, $\alpha_t \in [-\gamma, 1 + \gamma]$, and so nothing prevents $\alpha_t < 0$ or $\alpha_t > 1$, despite rarely happening for a small γ . Therefore, we must restrict $\alpha_t \in (0, 1)$.

4 AEnbMIMOCQR algorithm

In most cases, the distribution of blocks $B_t = \{(x_{(n_t-d+1):n_t}, x_{(n_t+1):(n_t+H)})\}_{t=1}^T$ proposed in Algorithm (2) are not i.i.d. nor exchangeable. That is, $\exists \pi : \{1, 2, \dots, T\} \rightarrow \{1, 2, \dots, T\}$ such that

$$\mathbb{P}\{(B_1, B_2, \dots, B_n) \in E\} \neq \mathbb{P}\{(B_{\pi(1)}, B_{\pi(2)}, \dots, B_{\pi(n)}) \in E\}. \quad (27)$$

Hence, in such cases MIMOCQR will not provide $1 - \alpha$ coverage. Therefore, it is key to draw some ideas from adaptive and dynamic methods to make it *asymptotic valid*. The idea is to improve Algorithm (2) by applying the following: a homogeneous ensemble learner; a sliding window of the *non-conformity scores* as in EnbPI and EnbCQR; sampling without replacement the in-sample *non-conformity scores* to speed up convergence; an adaptive scheme with a time-varying $(\alpha_t)_{t \in \mathbb{N}}$. Algorithm (3) encompasses every step highlighted here, in a comprehensive manner. The benefits of AEnbMIMOCQR over other probabilistic forecasting methods are depicted in Table (2).

Algorithm 3 Adaptive ensemble batch multi-input multi-output conformalized quantile regression (AEnbMIMOCQR)

Input: A training set $\{(B_i := x_{(n_i-d+1):n_i}, x_{(n_i+1):(n_i+H)})\}_{i=1}^T$, miscoverage rate α , a multi-output QR model $\hat{F}_\tau : \mathbb{R}^d \rightarrow \mathbb{R}^H$, an aggregation function ϕ , number of bootstrap models B , N observations to sample without replacement, a test set $\{(x_{(n_t-d+1):n_t}, x_{(n_t+1):(n_t+H)})\}_{t=T+1}^{T+T_1}$ with $x_{(n_t+1):(n_t+H)}$ revealed only after H timesteps.

Output: PIs $\{\hat{C}_{1-\alpha}^{(t)}(x_{(n_t+1):(n_t+H)})\}_{t=T+1}^{T+T_1}$

- 1: **for** $b \leftarrow 1, \dots, B$ **do**
- 2: Sample an index set $S_b = (i_1, \dots, i_T)$ from indices $(1, \dots, T)$
- 3: Compute $[\hat{F}_{\alpha/2}^b, \hat{F}_{1-\alpha/2}^b] \leftarrow (\hat{F}_{\alpha/2}(\{(B_i) \mid i \in S_b\}), \hat{F}_{1-\alpha/2}(\{(B_i) \mid i \in S_b\}))$
- 4: **end for**
- 5: $\epsilon_h \leftarrow \{\}, \quad \forall h \in \{1, \dots, H\}$
- 6: $\alpha_h \leftarrow \alpha, \quad \forall h \in \{1, \dots, H\}$
- 7: **for** $i \leftarrow 1, \dots, T$ **do**
- 8: $[\hat{x}_{n_i+1}^L, \dots, \hat{x}_{n_i+H}^L] \leftarrow \phi(\{(\hat{F}_{\alpha/2}^b(x_{n_i-d+1}, \dots, x_{n_i})) \mid i \notin S_b\})$
- 9: $[\hat{x}_{n_i+1}^U, \dots, \hat{x}_{n_i+H}^U] \leftarrow \phi(\{(\hat{F}_{1-\alpha/2}^b(x_{n_i-d+1}, \dots, x_{n_i})) \mid i \notin S_b\})$
- 10: Compute $\epsilon_h \leftarrow \epsilon_h \cup \{\max\{\hat{x}_{n_i+h}^L - x_{n_i+h}, x_{n_i+h} - \hat{x}_{n_i+h}^U\}\}, \quad \forall h \in \{1, \dots, H\}$
- 11: **end for**
- 12: Sample without replacement N elements from $\epsilon_h, \quad \forall h \in \{1, \dots, H\}$.
- 13: Compute $\hat{q}^{(h)} \leftarrow \text{Quantile}(\epsilon_h; 1 - \alpha_h), \quad \forall h \in \{1, \dots, H\}$
- 14: $\gamma \leftarrow 1/N$
- 15: **for** $t \leftarrow T+1, \dots, T+T_1$ **do**
- 16: $[\hat{x}_{n_t+1}^L, \dots, \hat{x}_{n_t+H}^L] \leftarrow \phi(\{(\hat{F}_{\alpha/2}^b(x_{n_t-d+1}, \dots, x_{n_t}))\}_{b=1}^B)$
- 17: $[\hat{x}_{n_t+1}^U, \dots, \hat{x}_{n_t+H}^U] \leftarrow \phi(\{(\hat{F}_{1-\alpha/2}^b(x_{n_t-d+1}, \dots, x_{n_t}))\}_{b=1}^B)$
- 18: Return $\hat{C}_{1-\alpha}^{(t)}(x_{n_t+h}) \leftarrow [\hat{x}_{n_t+h}^L - \hat{q}^{(h)}, \hat{x}_{n_t+h}^U + \hat{q}^{(h)}], \quad \forall h \in \{1, \dots, H\}$
- 19: **if** $t - T \equiv 0 \pmod{H}$ **then**
- 20: **for** $j \leftarrow t - H, \dots, t - 1$ **do**
- 21: Compute $\epsilon_h^{(*)} \leftarrow \max\{(\hat{x}_{n_j+h}^L - \hat{q}^{(h)}) - x_{n_j+h}, x_{n_j+h} - (\hat{x}_{n_j+h}^U + \hat{q}^{(h)})\}, \quad \forall h \in \{1, \dots, H\}$
- 22: $\alpha_h \leftarrow \alpha_h + \gamma(\alpha_h - \mathbb{1}\{x_{n_j+h} \in \hat{C}_{1-\alpha}^{(j)}(x_{n_j+h})\}), \quad \forall h \in \{1, \dots, H\}$
- 23: $\alpha_h \leftarrow \max\{0, \min\{\alpha_h, 1\}\}, \quad \forall h \in \{1, \dots, H\}$
- 24: $\epsilon_h \leftarrow (\epsilon_h - \{\epsilon_{h,1}\}) \cup \{\epsilon_h^{(*)}\}, \quad \forall h \in \{1, \dots, H\}$ and reset index of ϵ_h
- 25: **end for**
- 26: Compute $\hat{q}^{(h)} \leftarrow \text{Quantile}(\epsilon_h; 1 - \alpha_h), \quad \forall h \in \{1, \dots, H\}$
- 27: **end if**
- 28: **end for**

4.1 Generalization

So far, we have tackled conformal univariate time series forecasting; however, in many applications, there are also covariates beyond past observations of the target variable. Recurrent neural networks (RNNs) such as the long-short term memory (LSTM) [20] can be trained in a tensor $\mathbf{X} = \{(X_{(n_t-d+1):n_t}, X_{(n_t+1):(n_t+H)}^*)\}_{t=1}^T$ to learn an underlying function $F : \mathbb{R}^{d \times F_1} \rightarrow \mathbb{R}^{H \times F_2}$, where $F_1 \geq F_2$ are the number of input and output features, respectively. AEnbMIMOCQR can handle this scenario by simply training a LSTM network or other type of RNN with the *pinball loss*. Furthermore, in Algorithm (3), we must have $H \times F_2$ *non-conformity sets*, α_s , and \hat{q}_s , one per each feature and horizon as

$$\epsilon_{h,f}, \quad \forall h \in \{1, \dots, H\} \forall f \in \{1, \dots, F_2\}, \quad (28)$$

$$\alpha_{h,f}, \quad \forall h \in \{1, \dots, H\} \forall f \in \{1, \dots, F_2\}, \quad (29)$$

$$\hat{q}^{(h,f)}, \quad \forall h \in \{1, \dots, H\} \forall f \in \{1, \dots, F_2\}. \quad (30)$$

In the interest of space, we will not replicate Algorithm (3) for this case, even though the generalization to the multivariate time series case should be intuitive from these hints.

Method	Adaptive	Dynamic <i>non-conformity set</i>	Multi-output	Heteroscedastic
ARIMA	✗	✗	✗	✗
EnbPI	✗	✓	✗	✗
EnbCQR	✗	✓	✗	✓
MIMOCQR	✗	✗	✓	✓
AEnbMIMOCQR	✓	✓	✓	✓

Table 2: Summary of the probabilistic forecasting methods characteristics.

5 Experiments

We use the NN5 forecasting competition dataset as a benchmark. This dataset contains 111 time series, each one consisting of 791 daily cash demand observations at many ATMs at different locations in England. Probabilistic forecasting with ARIMA, EnbPI, EnbCQR, MIMOCQR, and our proposal AEnbMIMOCQR is performed on each series. All the code and data to reproduce the experiments can be found [here](#). As an evaluation criterion, we will look at coverage, median PIs width, and interquartile range (IQR). We apply min-max normalization on each time series to remove the scale dependence. Specifically, we use the following performance measures

$$\text{Median}^* = \frac{1}{111} \sum_{i=1}^{111} \text{Median}_i, \quad (31)$$

$$\text{IQR}^* = \frac{1}{111} \sum_{i=1}^{111} \text{IQR}_i, \quad (32)$$

$$\text{Coverage}^* = \frac{1}{111} \sum_{i=1}^{111} \text{Coverage}_i, \quad (33)$$

where Median_i , IQR_i and Coverage_i are the median PI width, IQR width, and coverage of the time series with $\text{id}=i$, respectively.

Table (3) showcases the number of deemed stationary time series via the Augmented Dickey-Fuller (ADF) test [21, 22] for different significance levels and a maxlag of 40.

Significance level	#series
0.1	92
0.05	84
0.01	67

Table 3: Number of stationary time series for different significance levels of the ADF test.

Besides ARIMA, which has an in-built linear autoregressive model with moving averages, we used a feedforward neural network (FFNN) [23] for all methods using the hyperparameters shown in Table (4). The unique difference is that EnbPI FFNN has a unique output neuron, which represents the single-output forecast optimized with mean squared error loss, while EnbCQR has 3 output neurons, each one minimizing a different *pinball loss* for $\alpha/2$, 0.5, and $1 - \alpha/2$ to get an estimated lower bound, forecast, and upper bound, respectively. MIMOCQR and AEnbMIMOCQR generalize the former with a total of $H \times 2$ output neurons since they do not require previous forecasts.

The parameters used in the evaluation phase are as follows. We set $T_1 = 400$, i.e., we leave the last 400 timesteps for evaluation, as seen in Fig.(1), and leave the remainder for training for $\alpha = 0.1$. For the multi-output methods, we set $H = 30$ and $d = 40$. We also use $d = 40$ for EnbPI and EnbCQR. The selection of d has a direct impact on the model's quality and therefore it should be carefully optimized. However, this optimization goes beyond the scope of this article. Nevertheless, we keep the coherence across models by choosing the same d among every model. Table (5) contains all the parameters for each method, whenever a parameter does not apply to the method in question we fill with "N.A.". For ARIMA, we also set $d = 40$, $q = 40$, and the order of differencing d^* is determined by the ADF test for a significance level of $\alpha = 0.1$. Be aware that using $T_1 = 400$ and $H = 30$ results in $\lfloor 400/30 \rfloor = 13$ updates on the *non-conformity set* for the dynamic methods (AEnbMIMOCQR, EnbPI, and EnbCQR).

Figures (1-4) show the variation of coverage across the last 400 timesteps for all methods, wherein AEnbMIMOCQR is clearly the best method in terms of *asymptotic validity*. We can also note that MIMOCQR and ARIMA tend to decrease coverage over time due to not accommodated distribution shifts. We can also verify that EnbPI converges faster than EnbCQR, yet not as fast as AEnbMIMOCQR. Figures (5-8) show the last 30-step ahead PIs for all conformal methods on time series with $\text{id}=4$, in which we see that EnbPI PIs are not heteroscedastic, and the coverage differences. In a broader scope, the performance measures uphold what can be inferred from the foregoing figures, i.e., AEnbMIMOCQR attains the best coverage (see Table 6). Moreover, AEnbMIMOCQR produces lower median PIs than EnbPI, on average, and its PIs vary more compared to EnbPI, on average, suggesting better adequacy for heteroscedastic time series and informative PIs to decision-making tasks. Recall that the small deviation seen in EnbPI PIs width is a mere consequence of updating the *non-conformity set* each $H = 30$ timesteps since PIs width is the same within the same batch.

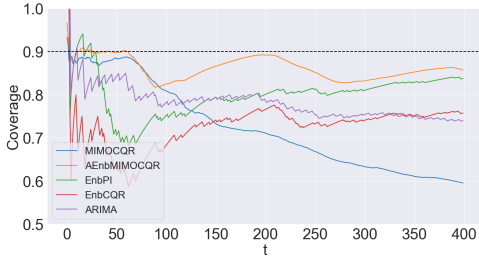


Figure 1: Coverage across timesteps. (Time series id=1)

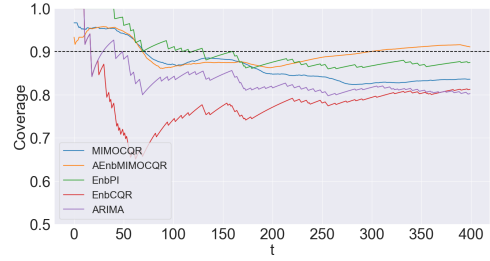


Figure 2: Coverage across timesteps. (Time series id=2)

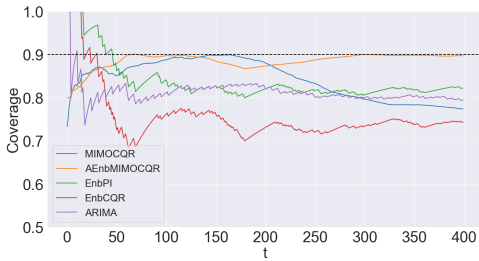


Figure 3: Coverage across timesteps. (Time series id=3)

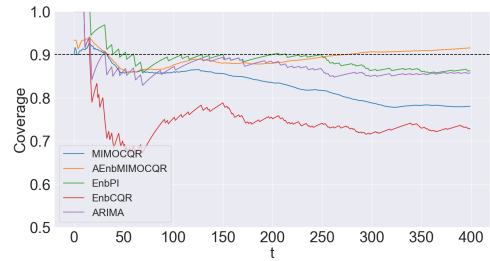


Figure 4: Coverage across timesteps. (Time series id=4)

Hyperparameter	Value
Epochs	1000
Batch size	100
Activation	ReLU
Dropout	0.1
First hidden layer	100 neurons
Second hidden layer	100 neurons

Table 4: Hyperparameters used for FFNN training.

Method	Model	B	N	T	T_1	d	H	α	ϕ
MIMOCQR	FFNN	N.A.	N.A.	322	400	40	30	0.1	N.A.
AEnbMIMOCQR	FFNN	10	100	322	400	40	30	0.1	mean
EnbPI	FFNN	10	N.A.	351	400	40	30	0.1	mean
EnbCQR	FFNN	10	N.A.	351	400	40	30	0.1	mean
ARIMA	ARIMA(40, d^* , 40)	N.A.	N.A.	391	400	40	N.A.	0.1	N.A.

Table 5: Probabilistic forecasting methods parameters.

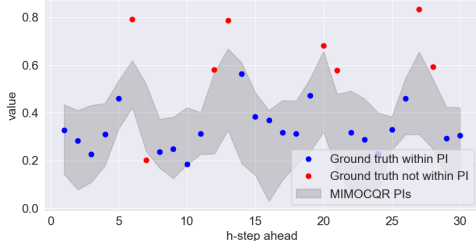


Figure 5: Last 30-step ahead PIs (MIMOCQR, id=4).

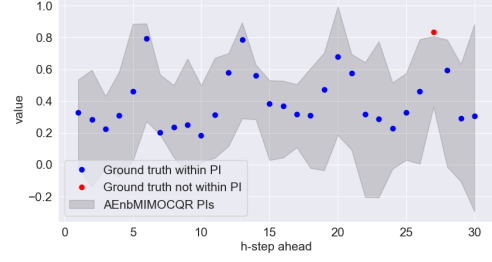


Figure 6: Last 30-step ahead PIs (AEnbMIMOCQR, id=4).

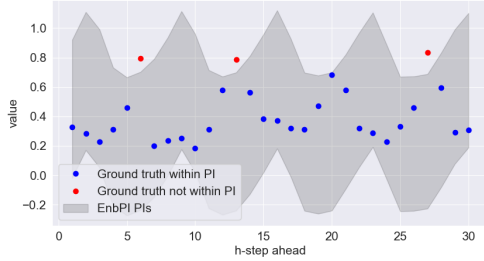


Figure 7: Last 30-step ahead PIs (EnbPI, id=4).

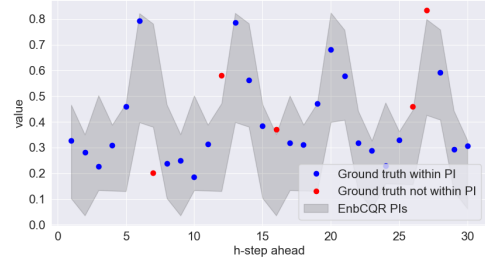


Figure 8: Last 30-step ahead PIs (EnbCQR, id=4).

Method	Coverage*	Median*	IQR*
MIMOCQR	0.844	0.372	0.109
AEnbMIMOCQR	0.887	0.493	0.350
EnbPI	0.876	0.593	0.010
EnbCQR	0.750	0.476	0.387
ARIMA	0.867	0.553	0.062

Table 6: Relative performance measures.

6 Conclusion

In this article, we proposed a new method called AEnbMIMOCQR for multi-step ahead conformal heteroscedastic time series forecasting that seeks to produce *asymptotic valid* PIs, based on the MIMO strategy, a dynamic *non-conformity set*, and an adaptive conformal inference scheme. Scale-independent performance measures applied on a reasonable scale benchmark containing several non-stationary and seasonal time series suggest that AEnbMIMOCQR completely outperforms competitive conformal methods in terms of coverage and PIs width. Although retraining the model from time to time can optimize the PIs width, AEnbMIMOCQR does not require data splitting as in ICP nor retraining the

model. Taking this strong evidence into consideration, henceforth AEnbMIMOCQR should be the state-of-the-art standard framework for conformal multi-step ahead heteroscedastic univariate and multivariate time series.

Acknowledgments

This work has been supported by COMPETE: POCI-01-0247-FEDER-039719 and FCT - Fundação para a Ciência e Tecnologia within the Project Scope: UIDB/00127/2020.

References

- [1] Vladimir Vovk, Alexander Gammerman, and Glenn Shafer. Algorithmic learning in a random world. 2005.
- [2] Glenn Shafer and Vladimir Vovk. A tutorial on conformal prediction. 2007.
- [3] Martim Sousa. Inductive conformal prediction: A straightforward introduction with examples in python, 2022.
- [4] Anastasios N. Angelopoulos and Stephen Bates. A gentle introduction to conformal prediction and distribution-free uncertainty quantification, 2021.
- [5] Shai Feldman, Stephen Bates, and Yaniv Romano. Conformalized online learning: Online calibration without a holdout set, 05 2022.
- [6] Isaac Gibbs and Emmanuel Candès. Adaptive conformal inference under distribution shift, 2021.
- [7] Margaux Zaffran, Aymeric Dieuleveut, Olivier Féron, Yannig Goude, and Julie Josse. Adaptive conformal predictions for time series, 2022.
- [8] Souhaib Ben Taieb, Gianluca Bontempi, Amir Atiya, and Antti Sorjamaa. A review and comparison of strategies for multi-step ahead time series forecasting based on the NN5 forecasting competition. *Expert Systems with Applications*, 39, 08 2011.
- [9] Souhaib Ben Taieb and Rob Hyndman. Recursive and direct multi-step forecasting: the best of both worlds. Monash Econometrics and Business Statistics Working Papers 19/12, Monash University, Department of Econometrics and Business Statistics, 2012.
- [10] Robert H Shumway and David S Stoffer. Arima models. In *Time series analysis and its applications*, pages 75–163. Springer, 2017.
- [11] Rob J Hyndman and George Athanasopoulos. *Forecasting: principles and practice*. OTexts, 2018.
- [12] Chen Xu and Yao Xie. Conformal prediction interval for dynamic time-series. In Marina Meila and Tong Zhang, editors, *Proceedings of the 38th International Conference on Machine Learning*, volume 139 of *Proceedings of Machine Learning Research*, pages 11559–11569. PMLR, 18–24 Jul 2021.
- [13] Martim Sousa, Ana Maria Tomé, and José Moreira. Improved conformalized quantile regression, 2022.
- [14] Yaniv Romano, Evan Patterson, and Emmanuel Candes. Conformalized quantile regression. In H. Wallach, H. Larochelle, A. Beygelzimer, F. d'Alché-Buc, E. Fox, and R. Garnett, editors, *Advances in Neural Information Processing Systems*, volume 32. Curran Associates, Inc., 2019.
- [15] Roger W Koenker and Gilbert Bassett. Regression quantiles. *Econometrica*, 46(1):33–50, 1978.
- [16] Roger Koenker and Kevin F Hallock. Quantile regression. *Journal of economic perspectives*, 15(4):143–156, 2001.
- [17] Vilde Jensen, Filippo Maria Bianchi, and Stian Norman Anfinsen. Ensemble conformalized quantile regression for probabilistic time series forecasting, 2022.
- [18] Victor Chernozhukov, Kaspar Wuthrich, and Yinchu Zhu. Exact and robust conformal inference methods for predictive machine learning with dependent data. *Proceedings of COLT 2018*, 2018.
- [19] Kamile Stankeviciute, Ahmed M. Alaa, and Mihaela van der Schaar. Conformal time-series forecasting. In M. Ranzato, A. Beygelzimer, Y. Dauphin, P.S. Liang, and J. Wortman Vaughan, editors, *Advances in Neural Information Processing Systems*, volume 34, pages 6216–6228. Curran Associates, Inc., 2021.
- [20] Sepp Hochreiter and Jürgen Schmidhuber. Long short-term memory. *Neural computation*, 9:1735–80, 12 1997.
- [21] David A. Dickey and Wayne A. Fuller. Distribution of the estimators for autoregressive time series with a unit root. *Journal of the American Statistical Association*, 74(366):427–431, 1979.
- [22] David A. Dickey and Wayne A. Fuller. Likelihood ratio statistics for autoregressive time series with a unit root. *Econometrica*, 49(4):1057–1072, 1981.

- [23] Ian J. Goodfellow, Yoshua Bengio, and Aaron Courville. *Deep Learning*. MIT Press, Cambridge, MA, USA, 2016.